Acta Crystallographica Section D
Biological Crystallography
ISSN 0907-4449

Refined structure of the FKBP12–rapamycin–FRB ternary complex at 2.2 Å resolution

Jun Liang,[a] Jungwon Choi[b] and Jon Clardy[a]*

[a]Department of Chemistry, Cornell University, Ithaca, New York 14853-1301, USA, and [b]Department of Chemistry, Suwon University, Kyunggi 445-773, South Korea

Correspondence e-mail: jcc12@cornell.edu

Received 7 August 1998
Accepted 9 November 1998

PDB Reference: FKBP12–rapamycin–FRB ternary complex, 2fap.

The structure of the FKBP12–rapamycin–FRB ternary complex has now been refined at 2.2 Å resolution. The cell-cycle arrest agent rapamycin binds FK506-binding protein (FKBP12) and the FKBP12–rapamycin binding (FRB) domain of FKBP12–rapamycin associated protein (FRAP) simultaneously, and the inhibition of FRAP is responsible for rapamycin's biological activity. The conformation of rapamycin in the ternary complex is very similar to that observed in the FKBP12–rapamycin binary complex, with an r.m.s. difference of only 0.30 Å. However, a slight (9°) rotation repositions the FRB-binding face of rapamycin in the ternary complex. There are extensive rapamycin–protein interactions and relatively few interactions between the two protein partners FKBP12 and FRB, these interactions mainly involving residues in the 40s and 80s loops of FKBP12 and α1 and α4 of FRB. The high-resolution refinement has revealed the crucial role of several buried waters in the formation of the ternary complex.

1. Introduction

The extraordinary natural products rapamycin (Sehgal *et al.*, 1975) and FK506 (Kino *et al.*, 1987) (Fig. 1) are potent immunosuppressive agents (reviewed by Schreiber, 1991). Both molecules bind with high affinity (0.2–0.4 n*M*, respectively) to the FK506-binding protein (FKBP12) (Harding *et al.*, 1989; Siekierka *et al.*, 1989) and inhibit its peptidyl–prolyl isomerase (PPIase) activity. The high-resolution structures of the FKBP12–rapamycin complex (Van Duyne, Standaert, Schreiber *et al.*, 1991) and the FKBP12–FK506 complex (Van Duyne, Standaert, Karplus *et al.*, 1991) reveal that both ligands have a very similar FKBP12-binding region, which includes the ester, pipecolinyl, cyclohexyl, pyran and tricarbonyl region (Fig. 1), and binds in a deep hydrophobic FKBP pocket comprised of conserved aromatic residues. The part of FK506 and rapamycin which projects away from FKBP has been termed the effector region (Van Duyne *et al.*, 1993) and the effector regions of FK506 and rapamycin bear little resemblance to each other (Fig. 1). Inhibition of FKBP12's PPIase activity is not responsible for immunosuppression and PPIase inhibitors are not immunosuppressive agents. Immunosuppression is caused by the ability of FKBP12–FK506/rapamycin to inhibit key portions in cytoplasmic signal transduction cascades. The FKBP12–FK506 complex, but not the FKBP12–rapamycin complex, inhibits the calcium-dependent phosphatase calcineurin (Liu *et al.*, 1991; O'Keefe *et al.*, 1992; Clipstone & Crabtree, 1992). The FKBP12–rapamycin complex, but not the FKBP12–FK506 complex, inhibits a 289 kDa protein named FK506-rapamycin associated protein

(FRAP) in humans (Brown *et al.*, 1994) and RAFT1 in rats (Sabatini *et al.*, 1994). Therefore, rapamycin and FK506 fall into a very limited group of cell-permeable molecules which generate a gain of function in their initial protein targets (Crabtree & Schreiber, 1996), this gain of function being attributable to the ability of the small-molecule ligand to simultaneously bind two proteins.

FRAP belongs to the ataxia telangiectasia mutant (ATM) family of high molecular-weight proteins which participate in cell-cycle progression, chromosome maintenance and repair, DNA recombination and cell-cycle checkpoints (Keith & Schreiber, 1995). At the C-terminal region, members of the family share varying degrees of homology to phosphatidylinositol (PI) kinases. FRAP is most highly related to two gene products from *S. cerevisiae*, TOR1 and TOR2 (Heitman *et al.*, 1991). Mapping of the minimal human FKBP12-rapamycin-binding domain (FRB domain) of FRAP indicates that a small, 90 amino-acid fragment (residues 2025–2114, K_d = 4.7 n*M*; Chen *et al.*, 1995) is sufficient to confer specific FKBP12 binding in a rapamycin-dependent fashion. Therefore, rapamycin is able to mediate the association of two small soluble proteins, FKBP12 and FRB, and this enforced association is being exploited by the use of rapamycin to control cellular processes such as gene transcription (Rivera *et al.*, 1996). The crystal structure of FKBP12–rapamycin in complex with the FRB domain (residues 2019–2112) has been solved by a combination of molecular replacement with isomorphous replacement for a single derivative ($HgCl_2$) plus anomalous scattering (SIRAS) at 2.7 Å resolution (Choi *et al.*, 1996). Here, we report the structure refined at 2.2 Å resolution and an analysis of interactions that are involved in this remarkable FKBP12–rapamycin–FRB ternary complex.

2. Experimental

2.1. Crystallization and data collection

Expression and purification of recombinant human FKBP12 (Van Duyne *et al.*, 1993) and the FRB domain of human FRAP (Chen *et al.*, 1995) have been described. After gel-filtration (Pharmacia HR12/6), FKBP12 was concentrated to 6 mg ml^{-1} and FRB was concentrated to 2 mg ml^{-1}. Protein concentrations were measured by UV absorption. FKBP12 was mixed with rapamycin (10 mg ml^{-1} in methanol) in a 1:3 molar ratio and the mixture was stored at 277 K overnight. The mixture was then passed through a 0.22 mm filter unit (Millipore) to remove the insoluble rapamycin. FRB was added to the FKBP12–rapamycin complex solution in a 1:1 molar ratio. The ternary complex thus made was stored in 20 m*M* Tris–HCl pH 8.0, 150 m*M* NaCl. Hanging drops containing equal amounts of the FKBP12–rapamycin–FRB ternary complex and the well solution (15–20% PEG 8000, 5–10% methylpentanediol, 100 m*M* Tris–HCl, pH 8.5) were set up at room temperature on an ice bucket and were stored at 277 K. Microseeding was used to ensure crystal growth, and crystals usually appeared two days after seeding and grew to maximum size in two to three weeks. A crystal with dimensions 0.8 × 0.4 × 0.2 mm was used for data collection. Data were collected at room temperature using two San Diego multiwire area detectors and a Rigaku RU-200 rotating-anode X-ray source (50 kV, 150 mA). The rod-shaped crystals belong to space group $P2_12_12_1$ with a = 46.3, b = 52.4, c = 102.0 Å, and one ternary complex forms the asymmetric unit. The solvent content is 51%. No measurements were deleted and Friedel pairs were averaged. The data were reduced using *SCALEPACK*. Statistics for the final data set are shown in Table 1.

2.2. Starting model and refinement

The 2.7 Å resolution structure was used as the initial model for least-squares refinement and simulated annealing in *X-PLOR* (Brünger, 1993). Graphical fitting (peptide-bond flip, side-chain conformational change *etc.*) was performed using the program *CHAIN* (Sack, 1988). Initially, the individual B values were restrained to 15.0 Å^2 and were varied only in the last cycles of refinement. Data from 8–2.2 Å were used for the refinement without bulk-solvent modification. Waters were added only after the restrained B-factor refinement of FKBP12–rapamycin–FRB was completed. Ordered waters were added if a peak appeared in the $F_o - F_c$ difference map with height greater than 3σ and the position of the peak implied at least one hydrogen bond within 4 Å, either to a protein atom or to another already defined water molecule. All residues of FKBP12 and FRB in the final model are located in the allowed regions of the Ramachandran plot, with

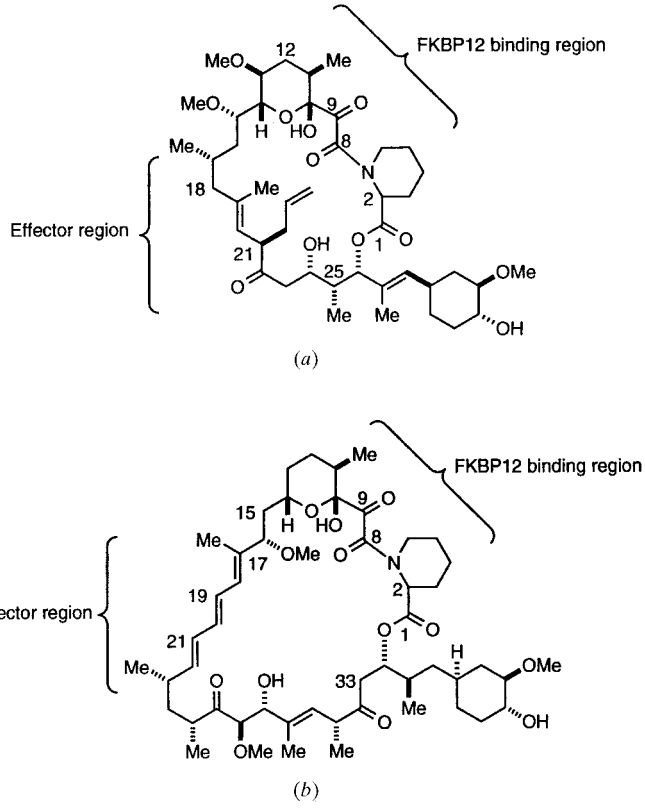

Figure 1
Chemical structures of (*a*) FK506 and (*b*) rapamycin, showing the regions interacting with FKBP12 and FRB or calcineurin (effector region).

Table 1
Data-collection and refinement statistics.

The final data set

Maximum resolution (Å)	2.2
Total number of unique reflections	12865
Number of observations	30805
with $I/\sigma < 1$	466
with $1 \leq I/\sigma < 2$	1271
with $2 \leq I/\sigma < 3$	2654
with $I/\sigma > 5$	21119
Completeness to 2.2 Å (%)	97.4
Completeness between 2.3 and 2.2 Å (%)	90.8
R_{sym} (I) (all reflections except single measurements) (%)	8.7
R_{sym} (I) between 2.3 and 2.2 Å (%)	27.0

Refinement

Maximum resolution (Å)	2.2
R factor (%)	19.6
R_{free} (10% of reflections excluded) (%)	26.5
Number of non-H atoms	1829
Protein atoms	1637
Rapamycin	66
Water	126
R.m.s. deviations from ideal geometry†	
Bond lengths (Å)	0.006
Bond angles (°)	0.94
Dihedral angles (°)	25.5
Improper angles (°)	1.4
Average B values (Å^2)	
All FKBP atoms	14.8
All FKB atoms	16.5
Rapamycin	7.3
Water	35.2
R.m.s. ΔB‡	2.8

† From the *X-PLOR* program package. ‡ Between covalently bonded atoms. B factors were refined using *X-PLOR*.

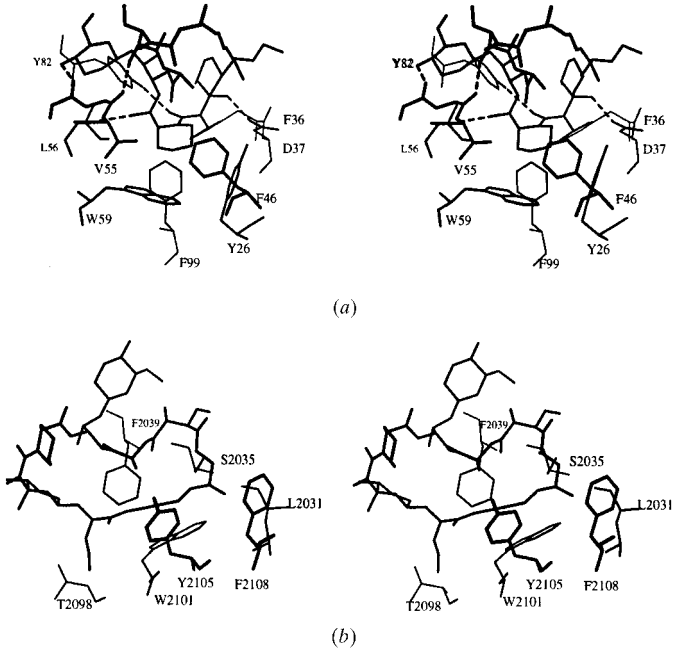

Figure 2
Stereoviews of (*a*) the rapamycin-binding pocket of FRB and (*b*) the rapamycin-binding pocket of FKBP12. Hydrogen bonds between rapamycin and FKBP12 are indicated by dashed lines, the ligand is in bold lines and the protein has light lines and residue labels.

Table 2
Protein–ligand interactions.

FRB–rapamycin

	Contacts less than 4 Å	
Ligand region	Protein residues (number of contacts)	Total contacts
C10–C14	Phe2039 (1)	1
C16–OMe	Thr2098 (1)	1
C17–C22	Ser2035 (3), Phe2039 (1), Trp2101 (1), Tyr2105 (6), Phe2108 (1)	12
C23–Me	Leu2031 (3), Ser2035 (2), Phe2108 (5)	10
C27–OMe	Glu2032 (1), Ser2035 (3), Arg2036 (3)	7
C29–Me	Phe2039 (3)	3
C34–C36	Phe2039 (2)	2
C37–C42	Gly2042 (2)	2

FKBP12–rapamycin

	Contacts less than 4 Å	
Ligand region	Protein residues (number of contacts)	Total contacts
C1	Val55 (4), Ile56 (3), Tyr82 (4)	10
C2–N7	Tyr26 (2), Phe46 (3), Val55 (1), Tyr59 (12), Tyr82 (1)	19
C8–C9	Tyr26 (1), Phe36 (3), Asp37 (4), Tyr82 (4), Phe99 (3)	15
C10–C14	Phe36 (2), Asp37 (6), Ile90 (1), Ile91 (2)	11
C28–C30	Glu54 (7)	7
C31 carbonyl	Phe46 (1), Asp54 (2), Val55 (1)	4
C34–C36	Tyr82 (4)	4
C37–C42	Gln53 (6), Glu54 (1), Val55 (3), Ile56 (4)	14

only Ala81 of FKBP12 in the generously allowed region. Refinement statistics are given in Table 1.

3. Results

3.1. Overall topology and protein–rapamycin interactions

The structures of rapamycin and FK506 have conventionally been divided into two regions (Fig. 1). The common FKBP-binding region interacts with FKBP, and small molecules with these structural features have PPIase activity. The effector regions of FK506 and rapamycin, which differ considerably (Van Duyne *et al.*, 1993), interact with calcineurin and FRAP (FRB), respectively. Rapamycin is at the center of the ternary complex and uses different faces to interact with FKBP12 and FRB. FKBP12 contains a twisted β-sheet (with five antiparallel β-strands) wrapped around a short α-helix. Rapamycin binds in a hydrophobic pocket formed between the β-sheet and the α-helix. Three loops – the 40s loop (a bulge in β5), the 50s loop (loop between β5 to α) and the 80s loop (loop between β2 and β3) – surround and contribute to the binding pocket. Interactions between rapamycin and FKBP12 in the ternary complex are very similar to those in the binary complex (see Table 2) and they have been analyzed in

Table 3
Intermolecular contacts and water-mediated interactions observed in the FKBP12–rapamycin–FRB ternary complex.

Intermolecular contacts between FRB and FKBP12 (<4.0 Å)

FKBP12 residue	FRB residue	Distance (Å)	Number of contacts
Lys44 CE	Arg2109 NH1	3.7	1
Phe46 CE2	Tyr2105 OH	3.9	1
Lys47 O	Tyr2105 OH	3.6	1
Thr85 OG1	Arg2042 CZ, NH1	4.0, 3.9	2
His87 ND1, CE1	Arg2042 NH2	3.3, 3.5	2
His87 CE1, NE2	Phe2039 CA, O, CD1	3.3–4.0	5
Pro88 CD, CG	Arg2042 CD, CG	3.8–4.0	3
Pro88 O	Val2094 CG2	3.5	1
Gly89 CA, C, O	Val2094 CG2	3.6–4.0	3
Ile90 CG1	Val2094 CG1	4.0	1
Ile90 CD1	Thr2098 CG2	3.7	1

Water-mediated interactions between FKBP12, FRB and rapamycin (<3.2 Å)

Water number	*B* factor (Å^2)	Residue in FKBP12 (contact distance, Å)	Residue in FRB (contact distance, Å)	Contacting water (*B* factor, Å^2) (contact distance, Å)
316	23.7	Lys47 N (3.1)	Tyr2105 OH (2.8)	397 (44.3) (2.7)
317	24.0	Lys47 O (2.7) Glu54 OE2 (3.0)	Tyr2105 OH (2.8)	
330	26.8	His87 ND1 (3.3)	Phe2039 O (2.6) Arg2042 NH2 (2.9)	
361	32.3	Arg42 NE (3.1)	Asp2102 OD2 (2.9)	368 (35.6) (3.0)
368	35.6		Asp2102 OD2 (3.3)	361 (32.3) (3.0)
397	44.3	Pro45 O (3.1)		316 (23.7) (2.7) 353 (31.3) (3.0)
353	31.3	Lys44 O (2.8) Arg42 NH1 (3.1)		397 (44.3) (3.0)
331	27.2	Rap108 O8 (3.0)	Glu2032 OE1 (3.2)	
377	37.4	Rap108 O9 (3.1) Rap108 O10 (2.9)	Gln53 O (2.9)	
424	56.5	Rap108 O7 (3.1)	Asp37 OD1 (3.1)	361 (32.3) (3.2)

detail (Van Duyne *et al.*, 1993). The pipecolinyl ring (C2–N7) makes the deepest penetration into the hydrophobic pocket of FKBP12, where it is surrounded by the conserved aromatic rings of Tyr26, Phe46, Trp59 and Phe99 (see Fig. 2*a*). The ester linkage and the dicarbonyl are also deeply buried, with both the C1 and C8 carbonyl groups making regular hydrogen bonds with FKBP12 and with the C9 carbonyl group protruding into a special pocket formed by the edges of Tyr26, Phe36 and Phe99. At the end of the FKBP12-binding domain, the pyran ring makes a number of contacts with FKBP12, and the C10 hydroxyl forms a hydrogen bond to the Asp37 side chain. At the other end of the FKBP12-binding region, the cyclohexyl ring also makes a number of contacts with FKBP12, and C40 OH group makes a hydrogen bond to the Gln53 main-chain O atom. C28 OH group is oriented towards FKBP12 and makes a hydrogen bond to Glu54 O. A total of 460 Å^2 (44%) of the solvent-accessible surface area of rapamycin is buried by FKBP12.

The FRB domain forms a four-helix bundle and the four helices are connected by short underhand loops (Choi *et al.*, 1996). A hydrophobic crevice, which is composed of conserved aromatic residues, is formed near the crossing point of α1 and α4. Rapamycin is bound in this crevice through the triene arm (C17–C24). The FRB crevice is much shallower than FKBP's binding pocket, and the interactions between rapamycin and FRB are completely hydrophobic. The triene arm projects into the crevice, making 12 contacts with residues Ser2035, Phe2039, Trp2101, Tyr2105 and Phe2108 (see Fig. 2*b*). The most deeply buried atom of rapamycin, the methyl attached to C23, fits into a tiny cavity between Leu2031 and Phe2108. The C23 methyl makes a total of ten contacts with FRB. In addition to these interactions, the C25–C34 region and the cyclohexyl ring appendage of rapamycin make 14 superficial hydrophobic contacts with FRB (see Table 2). A total of 340 Å^2 (33%) of the solvent-accessible surface area of rapamycin is buried by FRB.

3.2. Protein–protein interactions

Table 3 lists all the interactions between FRB and FRAP, including water-mediated interactions. Only the two loop regions of FKBP12, the 40s loop and the 80s loop, interact with FRAP. The 40s loop of FKBP12 contacts the end of the α4 helix of FRB. Interactions are mainly polar hydrogen bonds mediated by six water molecules. Only the main-chain atoms of residue Lys47 and side-chain atoms of Lys44 and Phe46 have van der Waals contacts with FRB directly, while residues Arg42, Lys44, Pro45, Lys47 and Glu54 also contact FRB through water-mediated bridges. The 80s loop interacts with the end of the α1 and the beginning of the α4 helices of FRB. Residues Pro88 and Ile90 of FKBP12, which have been identified as important residues for modifying the effects of both FK506 and rapamycin *via* site-directed mutagenesis (Yang *et al.*, 1993), contact Val2094 and Thr2098 of FRB through hydrophobic interactions. The side chain of His87 adopts two possible conformations: in one conformation it interacts with residue Phe2039 and in the other it forms a possible hydrogen bond with side-chain atoms of Arg2042 (see Table 3). In the FKBP12–FK506–calcineurin complex, the side chain of residue Ile90 adopts a very different conformation from that seen in the binary complex in order to fit into a hydrophobic patch formed by calcineurin (Griffith *et al.*, 1995). However, in the FKBP12–rapamycin–FRB ternary complex, Ile90 has the same orientation as in the FKBP12–rapamycin binary complex, making only one hydrophobic contact with Val2094 and one with Thr2098. Although the interactions between FKBP12 and FRB are limited, 400 Å^2 of solvent-accessible surface area are buried.

The importance of the 80s loop in the interactions of the ternary complex is illustrated by FKBP13 (Jin *et al.*, 1991) and FKBP25 (Galat *et al.*, 1991), two other members of the FKBP immunophilin family. Like FKBP12, FKBP13 and FKBP25 are PPIases with high affinities for rapamycin and FK506. They also share high sequence identities with FKBP12. However, none of them is able to mediate the immunosuppressive activity of FK506 or rapamycin (Abraham & Wiederrecht, 1996). Structures of FKBP13–FK506 (Schultz *et al.*, 1994) and FKBP25's FKBP12-homologous domain complexed with rapamycin (Liang *et al.*, 1996) have been determined. FKBP13 and FKBP25's FKBP12-homologous domains have been docked to the ternary complex by superimposing the main-chain atoms. In FKBP13, the Gly89/Pro89 change creates an unfavorable steric hindrance between Pro89 and Val2094. In FKBP25, the tip of the 80s loop (Q203–K207) forms a 3_{10} helix rather than the type II turn in FKBP12, which brings the region much closer to the regions around Val2094 in FRB, resulting in unfavorable steric clashes (Fig. 3). In contrast to the 80s loop, differences in the 40s loop in FKBP13 and FKBP25 would not interfere with FRB binding.

Neither the 40s nor the 80s loops are involved in any symmetry-related contacts in the crystal lattice of the ternary complex. In the FKBP12–rapamycin binary complex, the 80s loop is heavily involved in crystal-packing interactions while the 40s loop is not. An analysis of the *B*-factor plot indicates that the conformation of the 40s loop is greatly stabilized in the triple complex, with *B* factors dropping from 50 Å^2 to less than 20 Å^2 (Fig. 4). The 80s loop in both complexes has similar *B* factors (~20 Å^2) and thus presumably reflects stabilization through crystal packing or through interaction with FRB as well as the effects of ligand binding.

3.3. Comparison of rapamycin conformations in different states

The conformation of rapamycin in the ternary complex is very similar to its conformation in the binary complex, with an r.m.s. difference of 0.30 Å for the non-H atoms (Fig. 5). There were no planarity constraints for torsional angles around C18–C19 and C20–C21 during the structure refinements in both the ternary complex and the binary complex. In the final 2.7 Å structure of the ternary complex, rotations of −15° about C18–C19 and 37° about C20–C21 appeared to slightly disrupt the conjugation of the triene region (Choi *et al.*, 1996). However, in the 2.2 Å structure, C18–C19 and C20–C21 are more planar. The torsion angle is 179° about C18–C19 and 172° about C20–C21, which agree well with the torsion angle of 177° for C18–C19 and 170° for C20–C21 in the 1.7 Å binary crystal structure. In comparison, the torsion angles are 176 and 172° in the unbound crystalline state (Swindells *et al.*, 1978). The planarity of the triene arm of rapamycin is maintained in all experimentally determined structures.

The orientation of rapamycin relative to FKBP12 changes slightly in the ternary complex, resulting in a relatively large displacement of the triene region (Fig. 6). When the fitting includes rapamycin, FKBP12 main-chain atoms and side-chain atoms of residues contacting the pipecolinyl ring, rapamycin is rotated by approximately 9° relative to the body of FKBP12, resulting in tiny changes in the FKBP12-binding region but more substantial changes in the FRB-binding region, *i.e.* the small angular adjustment of rapamycin in the FKBP binding pocket is magnified by the long lever arm of the triene. The rotation is necessary for the triene region to fit into FRB. The methyl group attached to C23, the most deeply buried portion of rapamycin, rotates through a distance of 1.6 Å in order to fit into the crevice between Phe2108 and Leu2031. In order to verify that the rotation of rapamycin is not an artifact of the fitting scheme, we have superimposed various FKBP–rapamycin

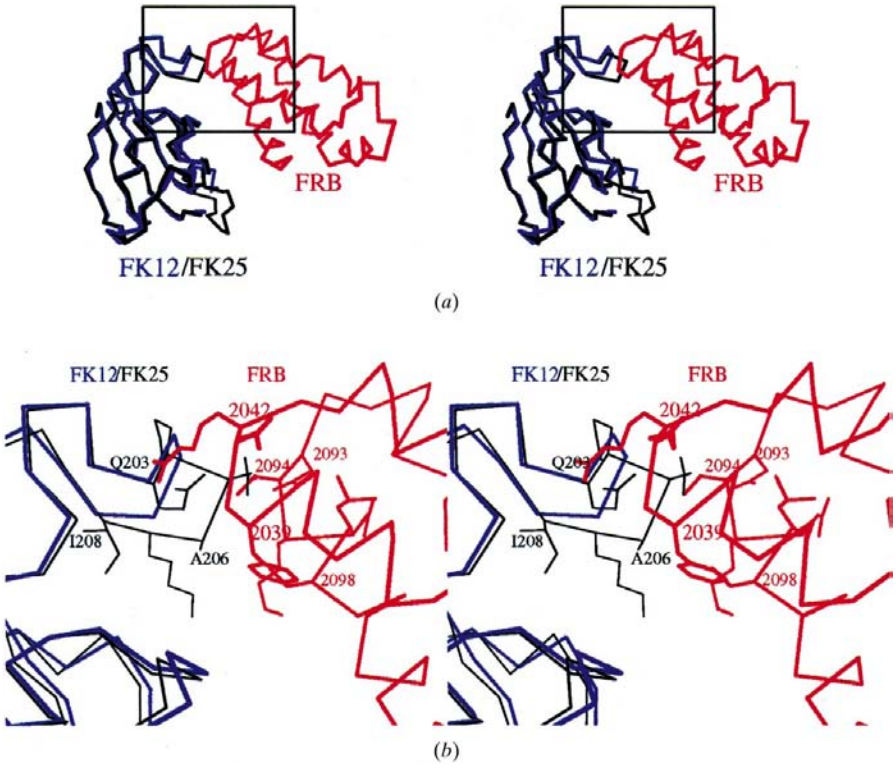

Figure 3
(*a*) Stereoview of the FKBP12 domain of FKBP25 (black) superimposed onto FKBP12 of the ternary complex (blue). FRB from the ternary complex is in red. Main-chain atoms of the FKBP25 C domain (Liang *et al.*, 1996) are superimposed onto the main-chain atoms of FKBP12 in the ternary complex. Rapamycin in the ternary complex is omitted from the drawing. (*b*) Enlarged view of the region framed in Fig. 3(*a*), showing unfavorable interactions between the end of the 80s loop of FKBP25 (side chains of residues Gln203–Ile208 and Cα trace of FKBP25) and the loops of FRB (side chains of 2039–2042 and 2093–2098 drawn in red). Main-chain traces of FRB (red) and FKBP12 (blue) are also shown. Rapamycin is omitted from the drawing.

crystal structures. FKBP25's FKBP12-homologous domain in complex with rapamycin has been determined by X-ray diffraction (Liang *et al.*, 1996). X-ray crystal structures of FKBP12 in complex with various rapamycin analogs have also been determined in different space groups (Luengo *et al.*, 1995). Rapamycin molecules have been exposed to many different crystal-packing environments in these binary complexes. Using the same fitting scheme as described above, rapamycin molecules of diverse binary complexes superimpose well with the rapamycin in the FKBP12–rapamycin binary complex and do not show the large displacement observed in fitting the ternary complex (data not shown). Therefore, we conclude that the observed rotation of rapamycin relative to FKBP12 is a real movement brought out by the FRB interaction. A similar rotation of FK506 has been observed in the FKBP12–FK506–calcineurin complex (Griffith *et al.*, 1995).

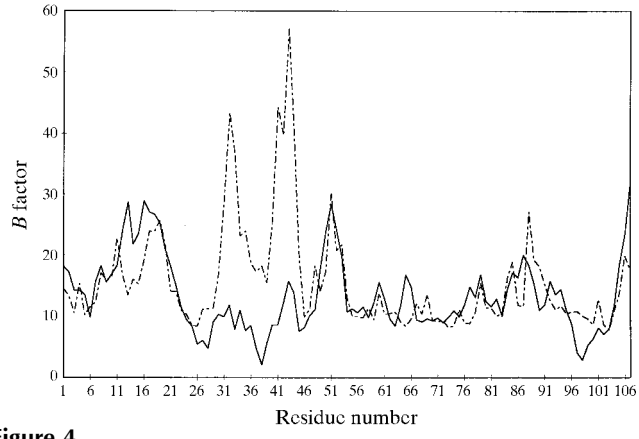

Figure 4
Average temperature factors (Å^2) per residue computed for FKBP12 main-chain atoms refined in the FKBP12–rapamycin–FRB ternary complex (solid line) and in the FKBP12–rapamycin binary complex (dashed line).

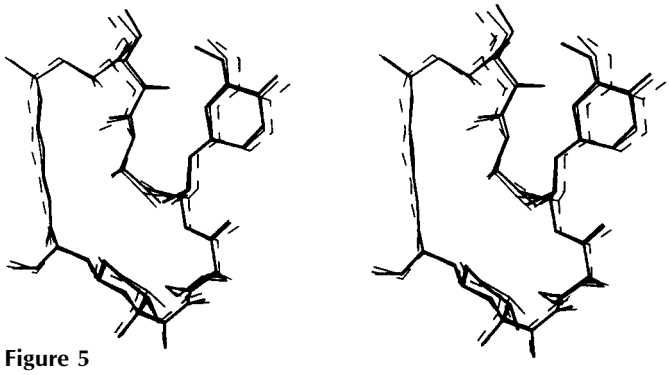

Figure 5
Stereoview of superposition of rapamycin conformations determined in the unbound solid state (dashed line; Swindells *et al.*, 1978), the FKBP12–rapamycin crystal structure at 1.7 Å (thin line; Van Duyne, Standaert, Schreiber *et al.*, 1991) and the FKBP12–rapamycin–FRB crystal structure at 2.2 Å (thick line). Only non-H atoms of rapamycin are superimposed.

Rapamycin alone cannot bind FRB efficiently, while rapamycin in complex with FKBP12 binds FRB tightly (Chen *et al.*, 1995). Conformations of rapamycin in the ternary complex, the binary complex and the unbound crystalline state (Swindells *et al.*, 1978) are very similar (see Fig. 4), and the r.m.s. deviation between rapamycin in the ternary complex and unbound rapamycin is 0.75 Å, which is slightly larger than that between the ternary complex and the binary complex (0.3 Å). An NMR study also indicates that rapamycin in DMSO solution adopts a conformation very similar to that observed in the rapamycin crystal structure and the complexed structure (Kessler *et al.*, 1993). In solution, exciton chirality studies have suggested that the triene region adopts a more rigid planar conformation after rapamycin is complexed with FKBP12 (Chen *et al.*, 1994), but the implications of this for complex formation are not clear. Upon binding FRB, the *B* factors of most atoms of rapamycin decrease. The cyclohexyl ring and the bridging region between the binding domain and the triene arm experience the largest stabilization as judged by *B*-factor analysis. The structural basis for the failure to measure any binding between rapamycin and FRB is not clear at present. It is likely that cooperative hydrophobic interactions of rapamycin, FKBP12 and FRB are important, even though the interactions between FKBP12 and FRB are more limited than those between rapamycin and FRB.

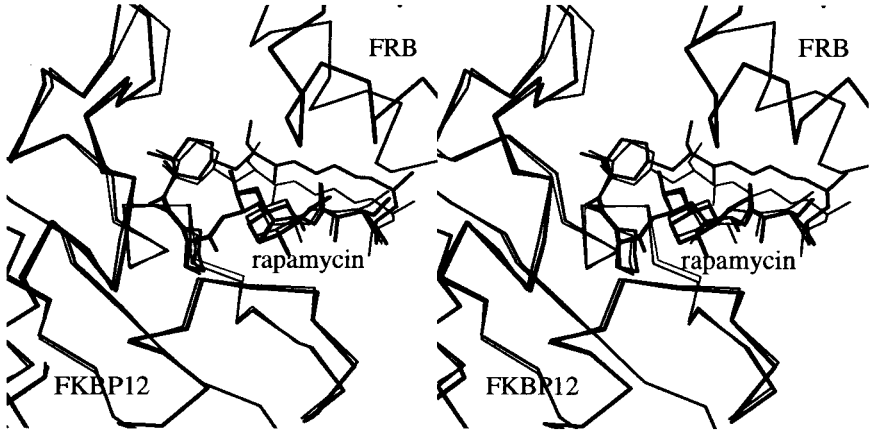

Figure 6
Conformations of rapamycin compared between the binary structure (Van Duyne, Standaert, Schreiber *et al.*, 1991; thin line) and in the ternary complex (thick lines). FKBP12 and FRB are drawn as Cα traces. The main-chain atoms of FKBP12, side-chain atoms of conserved aromatic residues in the binding pocket and non-H atoms of rapamycin are used in the superposition.

3.4. Comparison of FKBP12 in different structures

High-resolution crystal structures of uncomplexed FKBP12 (2.2 Å; Wilson *et al.*, 1995; Schultz & Clardy, 1998), the FKBP12–rapamycin complex (1.7 Å; Van Duyne *et al.*, 1991) and the FKBP12–rapamycin–FRB ternary complex (2.2 Å) have all been determined. Comparison of these three structures shows the FKBP12s to be very similar, with r.m.s. deviations of the main-chain atoms of only 0.3 Å between the ternary and the binary complex and 0.56 Å between the ternary complex and the uncomplexed FKBP12 (both calculations

Table 4
Water molecules in the ternary complex.

Categories: 1, water on surface of protein; 2, water in the protein inner space; 3, water in the packing interface (bridging symmetry-related molecules); 4, protein–protein water-mediated hydrogen bond; 5, protein–ligand water-mediated hydrogen bond; 6, no contact within 3.2 Å distance cutoff, but have contacts within 4.0 Å cutoff; 7, water networking (bridging other water molecules).

Number	Hydrogen bonded to	Category	Number	Hydrogen bonded to	Category
301	41 OD1, 35 NZ, 10 N†, W310†	3	364	18 NH1, W394	1
302	73 O, 3 O, 5 OE2, 75 OG1	3	365	2029 OE2, 2025 OE2	1
303	95 O, 82 N, W305, W419	2	366	2066 NZ, W326†	1
304	2022 N, 2025 OE1, 32 O†, W376†	3	367	2025 OE1, 32 OD1†, W318†	3
305	92 O, 94 N, 83 O, 95 N, W303	2	368	2102 OD2, W361	4
306	2075 O, W340	1	369		6
307	49 O, 54 N, 60 OE2, 52 N, 53 N	2	370	2065 O	1
308	2073 O, 2110 NH2, W388, W339†, 2052 OE2†	3	371	38 N, 38 O, 37 OD1, 42 NH2	1
309	31 O, W384, W336†	1	372	12 O	1
310	30 OE1, 67 OG, W301†, W327†	3	373	2041 OE2, 2043 ND2, W392	1
311	2110 O	3	374	2042 NH1	1
312	75 O	1	375	2029 OE1, 2029 OE2, 17 NZ†	3
313	2023 N, 2024 ND1, W314	2	376	32 O, W304†, 2025 OE2†	3
314	2064 OG1, 31 OE2†, W313	3	377	108 O10, 108 O9, 53 O	5
315	2087 NZ, 2083 OE1, W381	1	378	43 O, W358†	3
316	47 N, 2105 OH, W397	2	379	40 O, 43 OD1, W352, 6 OG1†, 6 N†, 4 O†	3
317	47 O, 54 OE2, 2105 OH	4	380	89 N, W416	1
318	32 OD1, W367†	1	381	W315	7
319	31 N, 96 O	1	382	2028 CB	1
320		6	383	2066 NZ	1
321	2089 SD, 2074 OH†, W343†	1	384	75 OG1, W309, W336†	1
322	100 O, 100 OD1	2	385	2049 OE1, W332	1
323	2059 OE1, 2055 O, 40 NE, 40 NH1	1	386	2109 O, W414	1
324	11 OD2, 13 NH2, W400	1	387	57 NH2	1
325	2073 O, 2077 OD1, 2077 OD2, 2077 N, W385†, W405	1	388	2110 NH2, W308, W339†	1
326	31 OE1, 31 OE2, W334†, W366†, 2065 N†, 2066 N†	3	389		6
327	35 NZ, W31O†	1	390	2043 ND2	1
328	7 O, W426	1	391	2042 NE, 2042 NH1	1
329	71 NH2, 102 OE1	1	392	2041 OE2, 2036 NH1, W373	1
330	2039 O, 2042 NH2, 87 ND1	4	393	2032 OE2	1
331	108 O8, 2032 OE1	5	394	W364	7
332	2045 O, 2049 OE1, W385	1	395	94 ND1	1
333	2058 O, 2071 ND2	1	396		6
334	2065 N, 96 OG1†, W337, W326	3	397	45 O, W316, W353	1
335	49 SD	1	398	W339, W421†	7
336	2021 N, 2021 O, 73 NZ†, W309†, W384†	3	399	104 O	1
337	96 OG1, W334†	1	400	W324	7
338	2044 N, 2045 N	1	401	2086 NH1, 2086 NH2, 2102 O, 2102 OD2	1
339	2052 OE1, 2052 OE2, W398	1	402	W341	7
340	2055 ND1, W306	1	403	2109 NH1, 2109 NH2, 2102 O, 2102 OD2	1
341	W426, W402	7	404	2053 O†, 2057 N†	1
342	W357	7	405	2072 O, 2071 O, 2075 N, 2076 N, W325, W332†	3
343	2074 OH, W321†	1	406	21 OG1, 107 OT	1
344	89 O	1	407	61 OE2, 57 NH1	1
345	2052 O, 2052 OE1	1	408	2068 OG1	1
346	55 O, 57 N	1	409		6
347	2072 NE2, 2088 OH†, W423	3	410	79 O, 57 NH2	1
348		6	411		6
349	91 O, 85 O	1	412	2059 OE1	1
350	2093 OD1, 2096 OD2	1	413	71 NH2	1
351	2049 O	1	414	2109 O, 2112 OT, W386	1
352	43 OD1, W379	1	415	40 NH2, 102 OE1	1
353	44 O, 45 O, 42 NH1, W397	7	416	W380	7
354	2053 CB	1	417	84 N, 85 OG1	1
355	47 NZ, 45 O	1	418	93 CG	1
356	94 ND1	1	419	95 O, W303	2
357	W342	7	420	65 NE2	1
358	2059 O, 2059 OE2	1	421	W398†	7
359	2026 SD, 2027 NE1	2	422	2038 OH, 87 NE2, 88 O	4
360		6	423	2072 NE2, W347	1
361	2102 OD2, 42 NE, W368, W424	4	424	108 O7, 37 OD2, 37 OD1, 42 NH2, W361	5
362	25 NE2, 43 O	1	425		6
363		6	426	W328, W341	7

† Atoms from symmetry-related molecules.

exclude residues 31–34). The largest difference is localized in residues Pro88 and Gly89 between the ternary and the binary complex and in residues Arg42 and Gly51 between the ternary complex and uncomplexed FKBP12 (see Fig. 7). Solution studies of FKBP12 (Michnick *et al.*, 1991) suggest that the 80s loop and the 40s loop do not have well defined solution conformations in the absence of ligand. It has also been reported that the tip of the 80s loop can be perturbed through the ligand binding and through crystal-lattice interactions (Wilson *et al.*, 1995). In the crystal structure of the binary complex, the 80s loop is extensively involved in crystal contacts, but in crystal structures of the ternary complex and uncomplexed FKBP12, the 80s loop is not involved in such contacts. Future work will be needed to define the various factors influencing the 80s loop.

3.5. Water molecules in the ternary complex

One of the main features of this higher resolution structure analysis is the 126 water molecules found during refinement. Only 23 water molecules were found in the 2.7 Å resolution structure. Most of the water molecules were found on the protein surfaces, but ten of them play an important role in protein–protein and protein–ligand interactions (Table 3). Seven of the water molecules are involved in protein–protein interactions bridging FKBP12 and FRB. Waters W316, W317, W353, W361, W368 and W397 form a hydrogen-bonding network between the 40s loop of FKBP12 and α4 of FRB. In addition, W330 bridges the 80s loop of FKBP12 and α1 of FRB. The protein–protein interactions in this complex consist mainly of water-mediated hydrogen bonds, and it is widely appreciated that bound water molecules are major contributors to the energetics of protein–protein complexes (Covell & Wallqvist, 1997).

There are three waters that bridge rapamycin and its protein partners. Two of them link rapamycin and FKBP: W377 mediates the hydrogen bonding between Gln53 and O10 of rapamycin, while W424 bridges Asp37 and O7 of rapamycin. One water plays an important role in the interaction between rapamycin and FRB. W331 mediates the hydrogen bond between Glu2032 of FRB and O8 of rapamycin. Since all of the other rapamycin–FRB interactions are hydrophobic, W331 is likely to be significant for rapamycin–FRB interactions. W424 forms a complex hydrogen-bonding network with other water molecules, a common feature in protein–ligand interactions (Poornima & Dean, 1995). These three water molecules provide some additional considerations for the development of new ligands, and rapamycin analogues with groups mimicking these waters could prove useful in the future. A summary of water–protein interactions is given in Table 4.

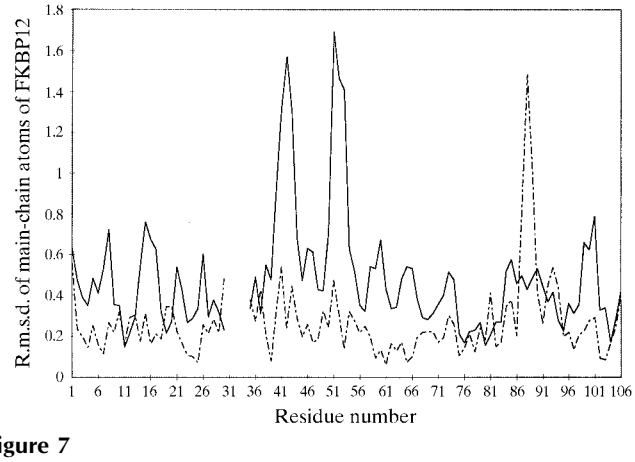

Figure 7
The root-mean-square deviation per residue computed for FKBP12 main-chain atoms between structures of the ternary complex and the binary complex (solid lines) and between the ternary complex and uncomplexed FKBP12 (dashed lines).

4. Conclusions

The 2.2 Å resolution structure of the FKBP12–rapamycin–FRB ternary complex reported here allows the structures of unliganded FKBP12, FRB, rapamycin and the binary FKBP12–rapamycin complex to be compared with the ternary complex on an equivalent basis. The 2.2 Å structure shows unequivocally that none of the molecules participating in the triple complex changes conformation upon ternary complex formation. The comparison between the binary (FKBP12–rapamycin) and ternary (FKBP12–rapamycin–FRB) complexes is the most informative. While rapamycin, the small-molecule glue holding the two proteins together, maintains its usual conformation, it does rotate through 9° relative to FKBP12 upon binding FRB. This rotation results in a very small shift of atoms in the FKBP12-binding pocket but a larger shift in the atoms interacting with FRB. The methyl group most deeply buried in the FRB-binding pocket is 1.6 Å away from its position in the binary complex. In FKBP12, only Pro88 and Gly89 move by more than 1 Å between the binary and tertiary complexes, and their position in the ternary complex is similar to that in unliganded FKBP12 (Schultz & Clardy, 1998). If the comparison is made between unliganded FKBP12 and FKBP12 in the ternary complex, both Arg42 and Gly52 move by more than 1 Å. Taken together, these comparisons suggest that the loop regions of FKBP12, especially the 80s loop and the 40s loop, are more flexible than other regions of FKBP12. The 2.2 Å structure also clarifies the role of water in complex formation. Seven well ordered waters are involved in protein–protein interactions and three of them moderate interactions of rapamycin with the proteins. Finally, the 2.2 Å structure gives a clearer definition of features that will be especially significant for structure-based drug design attempts to modify rapamycin.

This work was supported by NIH CA59201 with partial support for J. Choi from the Korea Research Foundation.

References

Abraham, R. T. & Wiederrecht, G. J. (1996). *Annu. Rev. Immunol.* **14**, 483–510.

Brown, E. J., Albers, M. W., Shin, T. B., Ichikawa, K., Keith, C. T., Lane, W. S. & Schreiber, S. L. (1994). *Nature (London)*, **369**, 756–758.
Brünger, A. T. (1993). *X-PLOR Version 3.1. A System for X-ray Crystallography and NMR.* Yale University Press, New Haven, Connecticut, USA.
Chen, J., Zheng, X. F., Brown, E. J. & Schreiber, S. L. (1995). *Proc. Natl Acad. Sci. USA*, **92**, 4947–4951.
Chen, Y., Zhou, P., Berova, N., Zhang, H. & Nakanishi, K. (1994). *J. Am. Chem. Soc.* **116**, 2683–2684.
Choi, J., Chen, J., Schreiber, S. L. & Clardy, J. (1996). *Science*, **273**, 239–242.
Clipstone, N. A. & Crabtree, G. R. (1992). *Nature (London)*, **357**, 695–697.
Covell, D. G. & Wallqvist, A. (1997). *J. Mol. Biol.* **269**, 281–297.
Crabtree, G. R. & Schreiber, S. L. (1996). *Trends Biochem. Sci.* **21**, 418–422.
Galat, A., Lane, W. S., Standaert, R. F. & Schreiber, S. L. (1991). *Biochemistry*, **31**, 2427–2434.
Griffith, J. P., Kim, J. L., Kim, E. E., Sintchak, M. D., Thomson, J. A., Fitzgibbon, M. J., Fleming, M. A., Caron, P. R., Hsiao, K. & Navia, M. A. (1995). *Cell*, **82**, 507–522.
Harding, M. W., Galat, A., Uehling, D. E. & Schreiber, S. L. (1989). *Nature (London)*, **341**, 758–760.
Heitman, J., Movva, N. R. & Hall, M. N. (1991). *Science*, **253**, 905–909.
Jin, Y. J., Albers, M. W., Lane, W. S., Bierer, B. E., Schreiber, S. L. & Burakoff, S. J. (1991). *Proc. Natl Acad. Sci. USA*, **88**, 6677–6681.
Keith, C. T. & Schreiber, S. L. (1995). *Science*, **270**, 50–51.
Kessler, H., Haessner, R. & Schüler, W. (1993). *Helv. Chim. Acta*, **76**, 117–130.
Kino, T., Hatanaka, H., Hashimoto, M., Nishiyama, M., Goto, T., Okuhara, M., Kohsaka, M., Aoki, H. & Imanaka, H. (1987). *J. Antibiot.* **40**, 1249–1255.
Liang, J., Hung, D. T., Schreiber, S. L. & Clardy, J. (1996). *J. Am. Chem. Soc.* **118**, 1231–1232.
Liu, J., Farmer, J. D. Jr, Lane, W. S., Freidman, J., Weissman, I. & Schreiber, S. L. (1991). *Cell*, **66**, 807–815.
Luengo, J. I., Yamashita, D. S., Dunnington, D., Beck, A. K., Rozamus, L. W., Yen, H. K., Bossard, M. J., Levy, M. A., Hand, A., Newman-Tarr, T., Badger, A., Faucette, L., Johnson, R. K., D'Alessio, K., Porter, T., Shu, A. Y., Heys, R., Choi, J., Kongsaeree, P., Clardy, J. & Holt, D. A. (1995). *Chem. Biol.* **2**, 471–481.
Michnick, S. W., Rosen, M. K., Wandless, T. J., Karplus, M. & Schreiber, S. L. (1991). *Science*, **252**, 836–839.
O'Keefe, S. J., Tamura, J., Kincaid, R. L., Tocci, M. J. & O'Neil, E. A. (1992). *Nature (London)*, **357**, 692–694.
Poornima, C. S. & Dean, P. M. (1995). *J. Comput. Aided Mol. Des.* **9**, 500–512.
Rivera, V. M., Clackson, T., Natesan, S., Pollock, R., Amara, J. F., Keenan, T., Magari, S. R., Phillips, T., Courage, N. L., Cerasoli, F. Jr, Holt, D. A., Gilman, M. (1996). *Nature Med.* **2**, 1028–1031.
Sabatini, D. M., Erdjument-Bromage, H., Lui, M., Tempst, P. & Snyder, S. H. (1994). *Cell*, **78**, 35–43.
Sack, J. S. (1988). *J. Mol. Graph.* **6**, 224–225.
Schreiber, S. L. (1991). *Science*, **251**, 283–287.
Schultz, W. L. & Clardy, J. (1998). *Bioorg. Med. Chem. Lett.* **8**, 1–6.
Schultz, W. L., Martin, P. K., Liang, J., Schreiber, S. L. & Clardy, J. (1994). *J. Am. Chem. Soc.* **116**, 3129–3130.
Sehgal, S. N., Baker, H. & Vezina, C. (1975). *J. Antibiot.* **28**, 727–732.
Siekierka, J. J., Hung, H. Y., Poe, M., Lin, C. S. & Sigal, N. S. (1989). *Nature (London)*, **341**, 755–757.
Swindells, D. C. N., White, P. S. & Findlay, J. A. (1978). *Can. J. Chem.* **56**, 2491–2492.
Van Duyne, G. D., Standaert, R. F., Karplus, P. A., Schreiber, S. L. & Clardy, J. (1991). *Science*, **251**, 839–842.
Van Duyne, G. D., Standaert, R. F., Schreiber, S. L. & Clardy, J. (1991). *J. Am. Chem. Soc.* **113**, 7433–7434.
Van Duyne, G. D., Standaert, R. F., Schreiber, S. L. & Clardy, J. (1993). *J. Mol. Biol.* **229**, 105–124.
Wilson, K. P., Yamashita, M. M., Sintchak, M. D., Rotstein, S. H., Murcko, M. A., Boger, J., Thomson, J. A., Fitzgibbon, M. J., Black, J. R. & Navia, M. A. (1995). *Acta Cryst.* D**51**, 511–521.
Yang, D., Rosen, M. K. & Schreiber, S. L. (1993). *J. Am. Chem. Soc.* **115**, 819–820.